Biochemical and Biophysical Research Communications 450 (2014) 1560–1567

Contents lists available at ScienceDirect

Biochemical and Biophysical Research Communications

journal homepage: www.elsevier.com/locate/ybbrc

Blockade of PDE4B limits lung vascular permeability and lung inflammation in LPS-induced acute lung injury

Ma Hongyan [a], Shi Jinghui [a], Wang Changsong [a], Guo Lei [a], Gong Yulei [a], Li Jie [c], Gong Yongtai [b], Yun Fengxiang [b], Zhao Hongwei [b], Li Enyou [a,*]

[a] Department of Anesthesiology, The First Affiliated Hospital of Harbin Medical University, Harbin 150001, People's Republic of China
[b] Department of Cardiovascular Medicine, The First Affiliated Hospital of Harbin Medical University, Harbin 150001, People's Republic of China
[c] Department of Anesthesiology, Sun Yat-Sen Memorial Hospital, Sun Yat-Sen University, Guangzhou 510000, People's Republic of China

ARTICLE INFO

Article history:
Received 27 May 2014
Available online 11 July 2014

Keywords:
PDE4B
Acute lung injury
LPS
Vascular barrier dysfunction

ABSTRACT

Acute lung injury (ALI), acute respiratory distress syndrome (ARDS), is actually involved in an ongoing and uncontrolled inflammatory response in lung tissues. Although extensive studies suggested that phospodiesterase type 4B (PDE4B) may be related to inflammation, the underlying cell biological mechanism of ALI remains unclear. To further investigate the mechanism how PDE4B take part in inflammatory response and the maintenance of vascular integrity, we established the experimental model of ALI in vitro and in vivo. In vitro, we found that Cilomilast, Diazepam and PDE4B knockout could potently inhibit the LPS-induced NF-κB activation and inflammatory response in multiple cell types, including lung epithelial cells (A549), pulmonary microvascular endothelial cells (PMVECs) and vascular smooth muscle cells (VSMCs). Besides, PDE4B deletion attenuated the LPS-induced ROS generation. In vivo, PDE4B deletion could attenuate the lung water content, histological signs of pulmonary injury and elevate the ratio of partial pressure of arterial O_2 to fraction of inspired O_2 (PaO_2/FIO_2 ratio). Additionally, PDE4B deletion reduced LPS-induced vascular permeability. Collectively, our results strongly indicates that PDE4B is a valid target for anti-ALI.

1. Introduction

Acute lung injury (ALI) is a complex syndrome with high morbidity and mortality [1–4]. And, its pathological changes were characterized by overwhelmling and uncontrolled inflammatory response [1–4,6] and pulmonary microvascular diffuse infiltration [4,6]. According to the concept, inflammation response and maintenance of vascular integrity are impotent regulatory elements for ALI. Indeed, pathological changes of ALI including the release of proinflammatory mediators such as tumor necrosis factor-α (TNF-α), vascular cell adhesion molecule-1 (VCAM-1), intercellular adhesion molecule-1 (ICAM-1), interleukin-8 (IL-8), monocyte chemotactic protein-1 (MCP-1), reactive oxygen species (ROS) and etc, [1–4]. All of those proinflammatory mediators' imbalance will lead to the deterioration of ALI. For instance, VCAM-1, ICAM-1 and members of other adhesion molecules are up-regulated under inflammatory condition. All the adhesion molecules can promote the inflammatory cells binding to the endothelial cells. And, this process is a critical pathological process in maintenance of vascular integrity and inflammatory response [4,6]. Moreover, the generation of proinflammatory mediators were regulated by activation of Nuclear Factor-κB pathway and oxidative stress. And, recently, extensive studies have shown that phospodiesterase type 4B (PDE4B) inhibitors can relieve inflammatory response by modulating cAMP activity in cell [5,7–9], animal [10,11] and human model [12,13]. Hence, NF-κB signaling pathway, oxidative stress and PDE4B may involved in regulation the pathological process of ALI.

Despite of considerable studies available, the underlying molecular mechanisms leading to LPS-induced ALI remain elusive. And this study was intended to illustrate the role of PDE4B in the regulation of inflammatory response of LPS-induced ALI.

2. Materials and methods

2.1. Antibodies and reagents

PDE4B antibody was purchased from Abcam (Cambridge, United Kingdom). PECAM-1, ICAM-2, IP_3R-1, CD11b, IACM-1, VACM-1, IL-8 and MCP-1 antibodies were obtained from Santa Cruz Biotech (Santa Cruz, CA). GAPDH antibody was purchased

* Corresponding author. Address: Department of Anesthesiology, The First Affiliated Hospital of Harbin Medical University, 23 Youzheng Street, Nangang District, Harbin City, Heilongjiang Province 150001, People's Republic of China.
E-mail address: lienyouhydyymzk@yeah.net (E. Li).

http://dx.doi.org/10.1016/j.bbrc.2014.07.024
0006-291X/

from Beyotime Institute of Biotechnology (Beyotime, China), siRNA interference reagent (sc-29528), siRNA Dilution Buffer (sc-29527), siRNA Transfection Medium (sc-36868), Control siRNA-A (sc-37007) and PDE4B siRNA (sc-45426), PDE4B shRNA Lentiviral Particles (sc-45426-V) and Control shRNA Lentiviral Particles-A (sc-108080) were purchased from Santa Cruz Biotech (Santa Cruz, CA). Fetal bovine serum (FBS), DMEM medium, RPMI-1640 medium and DMEM/F-12 medium were purchased from Gibco (Gibco, USA). Cilomilast (SML0733; purity ⩾ 95%, HPLC) and Diazepam power (X4628; purity ⩾ 98%, HPLC) were purchased from sigma (St. Louis, USA).

2.2. Cell isolation and culture

VSMCs were isolated by an enzymatic dissociation method and cultured as described previously [14]. Briefly, male 250–300 g Sprague–Dawley rats were anesthetized, and the aorta was dissected and soaked immediately in the Kreb's solution(constituents: NaCl 137 mM, KCl 5.4 mM, $CaCl_2$ 2.0 mM, $MgCl_2$ 1.1 mM, NaH_2PO_4 0.4 mM, Glucose 5.6 mM, $NaHCO_3$ 11.9 mM, 100 U/ml penicillin and 100 U/ml streptomycin). After adipose tissue and connective tissue were removed, the vessel was cut into pieces, and plated with DMEM/F12 medium which was composed of 20% fetal calf serum, 100 U/ml streptomycin, 100 U/ml penicillin, 25 U/ml heparin, 2 mM L-glutamine and 10 ng/ml ECGs in a humidified atmosphere of 5% CO_2 at 37 °C. Until cells migrated from the pieces, dispersed cells with 0.2% trypsin and 0.02% EDTA. The single-cell suspension was collected and subcultured with DMEM/F12 medium with 20% FBS and subcultured in a humidified atmosphere of 5% CO_2 at 37 °C.

Pulmonary microvascular endothelial cells (PMVECs) were isolated and cultured as described previously [15]. Briefly, wild-type C57BL/6 mice were anesthetized, unbroken lung tissues were obtained in ice-cold DMEM medium. Then removed lung lobes from DMEM and dissected residue tissue into pieces, digested with collagenase/dispase (C/D) solution and dispersed into single-cell suspension to obtain Mouse Lung Endothelial Cells (MLECs). MLECs were selected with anti-PECAM-1 antibody combing to Dynabeads using a Magnetic Particle Concentrator (MPC). These cells are cultured on gelatin-coated tissue culture dishes until cell were >80% confluent. At this moment, cells were further purified using Dynabeads coupled to anti-ICAM-2 antibody, then transferred them to a new DMEM medium containing 20% FBS and 100 U/ml streptomycin 100 U/ml penicillin and subcultured in a humidified atmosphere of 5% CO_2 at 37 °C.

A549 cells were purchased from the American Tissue Culture Collection (ATCC, USA). Cells were cultured in F-12K medium supplemented with 10% FBS, 5 U/ml heparin, 100 U/ml penicillin and 100 U/ml streptomycin in a humidified atmosphere of 5% CO_2 at 37 °C.

Mouse monocytes were isolated and cultured as described previously [16]. Briefly, wild-type C57BL/6 mice were anesthetized, and peripheral blood was harvested. Then peripheral blood mononuclear cells (PBMC) were obtained through centrifugal by using Nycoprep 1.077 A (AX-IS-SHIELD). Monocytes were selected with CD11b antibody using a magnetic activated cell sorting system (Miltenyi Biotech), then transferred them to a new DMEM medium containing 20% FBS and 100 U/ml streptomycin and 100 U/ml penicillin and subcultured in a humidified atmosphere of 5% CO_2 at 37 °C.

2.3. Drug treatment

When performing drug treatment, Cilomilast and Diazepam were first added to the culture medium in a eppendorf tube and mixed thoroughly, respectively. The cells were seeded in 35 mm petri dish with normal growth medium for 6 h and then added the medium already mixed with previously mentioned drugs. Removal of the cultivate medium and washed with PBS for twice, then switched into normal growth conditions and subcultured for 24 h. Those cells were collected and used for the following study.

2.4. Small interfering RNA transfection

The Oligonucleotide sequences of siRNA targeting for PDE4B (sc-45426) was synthesized by Santa Cruz Biotech and Control siRNA-A (sc-37007) was used as negative control. Control siRNA-A consists of a scrambled sequence that will not lead to the specific degradation of any known cellular mRNA. The siRNA and negative control were transfected transiently according to the manufacturer's protocol, respectively [17]. Briefly, 1×10^5 PMVECs were seeded in 35 mm petri dish with normal growth DMEM medium supplemented with 20% FBS. And then, incubated the cells at 37 °C in a CO_2 incubator until the cells were 80% confluent. The siRNA was diluted in 100 μl siRNA Transfection Medium (sc-36868) without serum (the final siRNA concentration was 40 nM). 6 μl of siRNA Transfection Reagent (sc-29528) was diluted in 100 μl siRNA Transfection Medium. Then added the siRNA duplex solution directly to the dilute Transfection Reagent into a eppendorf tube. Kept the mixture mixing gently and incubated the mixture for 25 min, then added to the cells in quiescent state and incubation for 6 h in a humidified atmosphere of 5% CO_2 at 37 °C. Then removal of the transfection mixture, switched into normal growth conditions and subcultured for 24 h. Those cells were collected and used for the following study.

2.5. NF-κB activity assay

NF-κB Activity was determined by Dual luciferase assay as described previously [14,16,18]. Briefly, NF-κB promoter was cloned into the pGL2-basic luciferase reporter (Promega, USA). Meanwhile, cells were seeded in 60 mm petri dish for 6 h, then treated with PDE4B inhibitors or small interfering RNA as mentioned above. And then, all the cells were subcultured and stimulated with or without 2 μg/ml of LPS for 24 h. Finally, the already processed cells were co-transfected with Reporter plasmid (Luc-NF-κB) or pGL2-basic luciferase reporter and Renilla luciferase plasmid (pRL-TK) using FuGENE6 Transfection Reagent(Roche) for 2 h. Cell extracts Luminescence were examined by a luciferase counter (Infinite F500 mMulti Reader, TECAN). The relative luciferase activity was calculated by normalizing NF-κB promoter driven firefly luciferase activity to control Renilla luciferase activity.

2.6. ROS assay

Superoxide release from cells were measured using the superoxide-sensitive dye DHE as previously described [19]. PMVECs were stimulated with or without 2 μg/ml of LPS for 24 h, then washed with PBS twice and incubated with 5 μM DHE for 30 min, and then fixed with acetone and methanol (1:1) for 10 min. Superoxide release images were detected using confocal imaging system and the total fluorescence integrated density were examined using Image J Software.

2.7. Generation of stable PDE4B KO mice and animal experiments

To delete PDE4B in vivo, C57BL/6 mice were implemented to inject with PDE4B shRNA Lentiviral Particles (sc-45426-V;100MOI/kg) or Control shRNA Lentiviral Particles-A (sc-108080; 100 MOI/kg) via tail vein route every day for 30 days.

PDE4B protein expression was examined by immunoblotting using GAPDH as loading control.

For systemic administration, mice were randomly divided into five groups. Control group (administrated with an equal volume vehicle DMSO via an i.p. route every day), Cilomilast group (administrated with 10 mg/kg via an i.p. route every day), Diazepam group (administrated with 10 mg/kg via an i.p. route every day), Lenti-PDE4B KO mice group and Lenti-Ctrl-shR mice group. Six mice were used for each group. And then all mice were anesthetized and intratracheally inoculated with LPS (*Escherichia coli* serotype 055:B5, 100 μg/kg; Sigma) for 6 h.

2.8. Permeability assay

In vitro, for permeability assay [4,6], PMVECs were seeded into culture inserts(pore size 3 μm; Corning Biosciences). The cells were stimulated with or without 2 μg/ml of LPS for 24 h. And then loaded with dextran-FITC to the upper chamber for 30 min. Finally, diffusion was quantified by measuring fluorescence units in the lower chamber.

In vivo, albumin was employed to assess the lung vascular permeability [6]. Briefly, LPS (2 μg/ml) was administered retroorbitally into the vasculature of wild-type C57BL/6 mice (WT ctrl), Lenti-PDE4B KO mice (Lenti-PDE4B) and Lenti-Ctrl-shRNA mice (Lenti-Ctrl-shR) for 30 min, respectively. Then, Evans blue-labeled albumin (20 mg/kg) was injected retro-orbitally to mice. 1 h later, mice were anesthetized and blood was obtained from the right ventricle and plasma was separated. Lung lysates and plasma were incubated with 2 volumes of formamide for 18 h at 60 °C and centrifuged at 5000×*g* for 30 min. Spectrophotography was adopted to analyze using the optical density of the supernatant. EBA extravasation was calculated and reflexed indirectly lung vascular permeability.

2.9. PaO_2/FIO_2 ratio assay

The PaO_2/FIO_2 ratio was determined by Blood gas analysis in the experiment. Briefly, mice were anesthetized, arterial blood were obtained via aorta puncture. Then, the arterial partial pressure of oxygen was measured with an i-STAT 300 Analyzer(Abbott Point, Canada).

2.10. Lung wet/dry ratios [1–4,6]

Wet-dry proportion method was employed to determined lung tissue edema. Briefly, the exteriorized newly lung lobes in each group were weighed, subsequently dried them for 48 h in an oven at 60 °C and weighed.

2.11. Monocyte adhesion assay [14,16]

PMVECs were pretreated with Cilomilast, Diazepam and PDE4B siRNA transfection. Then the cells were stimulated with 2 μg/ml of LPS for 24 h. Mouse monocytes were labeled with 2 μM Calcein-AM and incubated for 30 min. Finally, added the Calcein-AM labeled monocytes to already processed PMVECs and co-incubation for 2 h at 37 °C, 5% CO_2. The non-adherent cells were removed by gently washed with PBS. Given 2 ml PBS into each dish and images were captured with laser confocal scanning microscopy with an excitation wavelength of 485 nm and emission at 530 nm.

2.12. Measuring cytokines

The levels of TNF-α, IL-8 and MCP-1 were measured in BAL fluid (bronchoalveolar lavage fluid) from mice using ELISA kits (R&D Systems, Minneapolis, USA), according to the manufacturer's instructions.

2.13. PMN recruitment analysis

Lung inflammatory cells were measured with PMN recruitment analysis [4,14]. Briefly, sterilized PBS was carefully perfused into the lungs and then sucked slowly via a cannula that had been inserted into the trachea. The numbers of total and differential cells from BAL were stained with Hemacolor (Merck Serono Co., China) after cytocentrifugation.

2.14. Western blot analysis

Western blot analysis was performed as described previously [14,20]. Briefly, Frozen adult mouse lung tissues or isolated cells were collected, rinsed with ice-cold PBS. Cells were homogenized in lysis buffer (P0013, Beyotime, Jiangsu, China) and 1% protease inhibitor (cocktail: CalbioChem, Darmstadt, Germany) for 30 min. Tissues were homogenized in lysis buffer and 1% protease inhibitor and lysates using tissue homogenizer. And, the protein was extracted by centrifugation at 12,000×*g* for 12 min at 4 °C. Protein concentration was detected by BCA assay (Beyotime, Jiangsu, China). Equal amounts of total protein was separated by 8–12% SDS–PAGE and transferred to PVDF membranes (Immobilon-P, Millipore). The membranes were blocked at room temperature for 45 min in 5% non-fat milk (10 mM Tris pH 7.5, 150 mM NaCl, 0.1% Tween 20, 5% non-fat milk), then incubated them for 2 h at room temperature initially with IACM-1, VACM-1, IL-8, MCP-1 and PDE4B antibodies, and then incubated with the appropriate secondary peroxidase conjugated antibodies. Blots were developing with enhanced chemiluminescence substrates (Beyotime, Jiangsu, China) and then visualized by exposure to Kodak X-ray film. Integrated optical density of target bands was accurately determined by the Image-J gel analysis system.

2.15. Histological analysis [1–4,12,14,16]

Paraffin-embedded lung tissues were sliced into 6 μm sections and collected for histological analysis. Dissected lung was inflated and fixed with 10% formaldehyde, then embedded in paraffin. And lung tissues sections were stained with H&E to delineate the inflammatory response and pathological changes in lung tissue.

2.16. Statistical analysis

Data were represented as means ± SD. Statistical significance was assessed by Student's *t* test or ANOVA-test. The *p* values less than 0.05 was considered significant.

3. Results

3.1. Decreased of PDE4B inhibits LPS-induced NF-κB activation and ROS generation

Massive researches have proved that NF-κB pathway was involved in inflammatory response [8,14,16], hence, we investigated whether PDE4B blockers inhibited inflammatory response by inhibiting the activity of NF-κB. We first examined the effects of Cilomilast and Diazepam on LPS-induced NF-κB activity by using a NF-κB-luciferase reporter plasmid transiently transfected in multiple cell types, respectively. The data showed that Cilomilast and Diazepam inhibited LPS-induced NF-κB activation and chemotactic activity in lung epithelial A549 cells (Fig. 1A and D), Pulmonary endothelial PMVECs cells (Fig. 1B and E) and Vascular

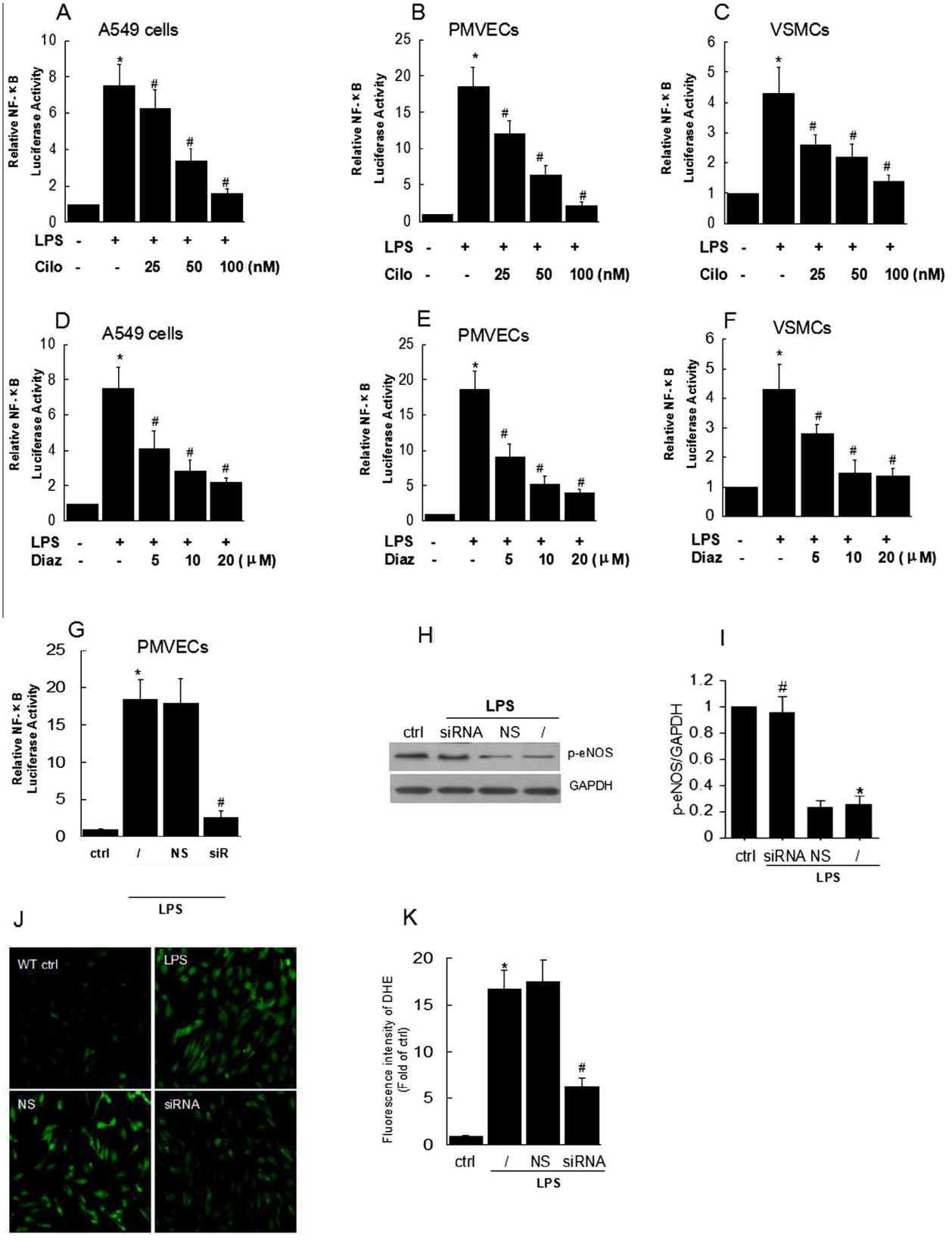

Fig. 1. PDE4B deletion inhibited LPS-induced NF-κB-dependent promoter activity in a variety of cell types and inhibited LPS-induced ROS generation. (A–C) Cells were pretreated with Cilo. (D–F) Cells were pretreated with Diaz (mean ± SD, $^{*}P < 0.05$ vs. control; $^{\#}P < 0.05$ vs. LPS alone; $n = 4$). (G) PMVECs were transfected with negative siRNA (NS) or PDE 4B siRNA (siR) (mean ± SD, $^{*}P < 0.05$ vs. control; $^{\#}P < 0.05$ vs. NS; $n = 3$). (H) Representative image of p-eNOS expression. (I) Statistical analysis of p-eNOS (Data represent mean ± SD, $^{\#}P < 0.05$ vs. LPS alone; $^{*}P < 0.05$ vs. siRNA. $n = 3$). (J) Representative images of ROS production by DHE staining. (K) Statistical analysis of the fluorescence intensity. (Data represent mean ± SD, $^{*}P < 0.05$ vs. siRNA; $^{\#}P < 0.05$ vs. alone. $n = 3$).

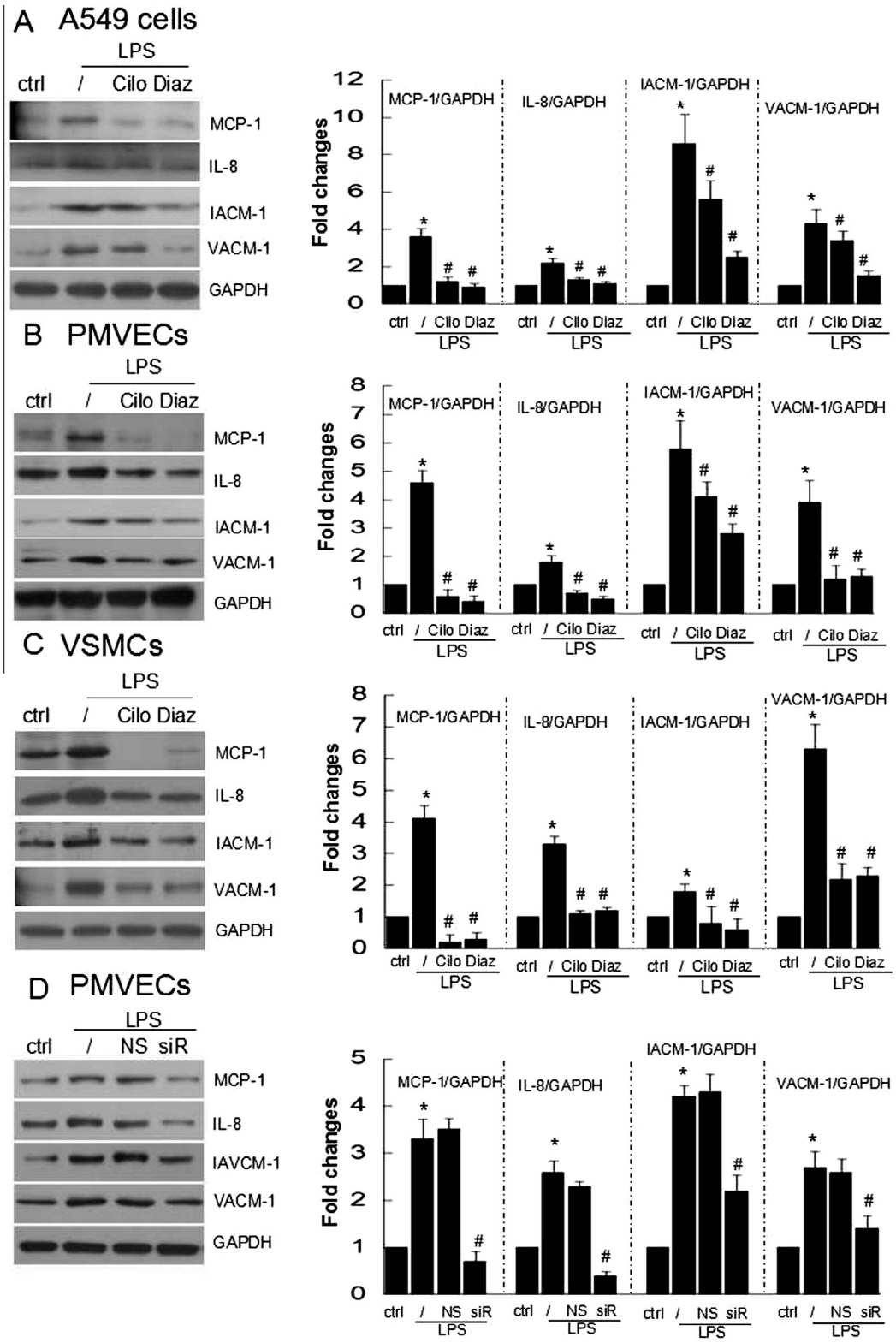

Fig. 2. PDE4B deletion inhibited LPS-induced expression of proinflammatory cytokines in a variety of cell types. (A–C) Cells were pretreated with 50 nM Cilomilast (Cilo) or 10 μM Diazepam (Diaz) for 2 h, then the cells were treated with LPS (2 μg/ml) for 24 h. Cells were then lysed and detected by Western Blot assay. (A) A549 cells. (B) PMVECs. (C) VSMCs (Bars represent mean ± SD, $^{*}P < 0.05$ vs. control; $^{\#}P < 0.05$ vs. LPS alone; $n > 3$). (D) PMVECs were transfected with negative siRNA (NS) or PDE4B siRNA (siR) (Bars represent mean ± SD, $^{*}P < 0.05$ vs. control; $^{\#}P < 0.05$ vs. NS; $n > 3$).

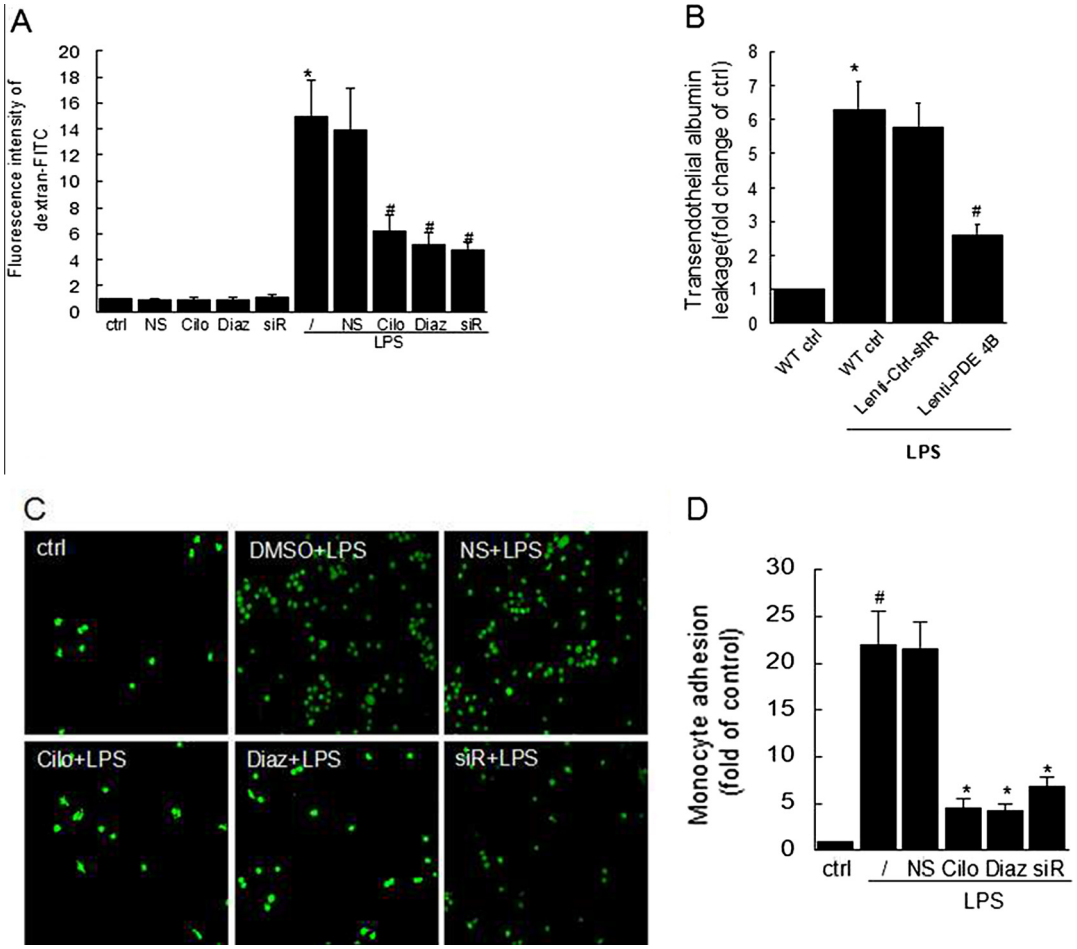

Fig. 3. Blockade of PDE4B limited LPS-induced lung vascular permeability. (A) Quantification of dextran-FITC fluorescence was used to measure the change of cell membrane permeability (Bars represent mean ± SD, $^{*}P < 0.05$ vs. control; $^{\#}P < 0.05$ vs. LPS alone. $n = 3$). (B) Quantification of EBA fluorescence was to described the transendothelial leakage (Bars represent mean ± SD, $^{*}P < 0.05$ vs. WT control; $^{\#}P < 0.05$ vs. Lenti-Ctrl-shR. $n > 3$). (C and D) Adhesion of calcein-labeled mouse monocytes to PMVECs which treated with Cilo, Diaz or transfected with negative siRNA (NS) or PDE4B siRNA (siR) (Bars represent mean ± SD, $^{*}P < 0.05$ vs. LPS alone; $^{\#}P < 0.05$ vs. control. $n = 3$).

Smooth Muscle VSMCs cells (Fig. 1C and F), respectively. To further investigate whether PDE4B directly involved in regulating the activity of NF-κB, PDE4B knockout was employed and NF-κB-dependent reporter gene luciferase activity was examined in PMVECs. As is shown in Fig. 1G, after transfected with siRNA of PDE4B followed by stimulation with 2 μg/ml of LPS for 24 h, the NF-κB activity decreased significantly. To further investigate whether oxidative stress was involved in the pathological process, we examined the ROS generation and the phosphorylation of eNOS. And we found that PDE4B deletion attenuated the LPS-induced ROS generation (Fig. 1H and I), and promoted LPS-inhibited p-eNOS activity (Fig. 1J and K) in PMVECs.

3.2. Suppression of PDE4B inhibites LPS-induced proinflammatory cytokines

We further investigated whether PDE4B blockers inhibits LPS-induced NF-κB activation involved in up-regulation of proinflammatory cytokines. Cells were pretreated with Cilomilast or Diazepam for 2 h before treated with or without LPS(2 μg/ml) for 24 h in the continued presence of Cilomilast and Diazepam, respectively. The proteins expression of IL-8, MCP-1, IACM-1 and VACM-1 were detected by Western Blot analysis. We found that Cilomilast or Diazepam inhibited the expression of LPS-induced proinflammatory cytokines (Fig. 2A–C), respectively. Simultaneously, PMVECs pretreated with PDE4B siRNA demonstrating a lower expression of proinflammatory cytokines (Fig. 2D). And, the expression of PDE4B was detected by Western Blot analysis. As shown in Fig. S1A, the Cilomilast, Diazepam and PDE4B siRNA inhibited the expression of PDE4B.

3.3. Blockade of PDE4B limits lung vascular permeability

To investigate the role of PDE4B in lung vascular permeability, we generated experimental model of ALI in cells and animals. We confirmed that LPS challenge significantly increased the membrane permeability in vitro (Fig. 3A) and in vivo (Fig. 3B). We also found that when PMVECs were treated with Cilomilast, Diazepam and PDE4B siRNA, the expressions of ICAM-1 and VCAM-1 were decreased obviously compared with the untreated group (Fig. 2D) under LPS stimulation. Meanwhile, LPS-induced adhesion of mouse monocytes to PMVECs were also reduced in PDE4B deletion (Fig. 3C and D).

3.4. Blockade of PDE 4B inhibits lung inflammatory response in vivo

To explore the physiological significance role of PDE4B, we investigated effect of PDE4B on LPS challenge inflammatory responses in vivo. The expression of PDE4B was decreased in Lenti-PDE4B KO mice or mice treated with PDE4B blockers (Fig. 4C and D). And we evaluated the effects of PDE4B blockers or PDE4B shRNA Lentiviral Particles on inflammation induced by intratracheal inoculation with LPS (100 μg/kg) for 6 h and determined using HE staining, as shown in Fig. 4A, lung architecture of ALI mice

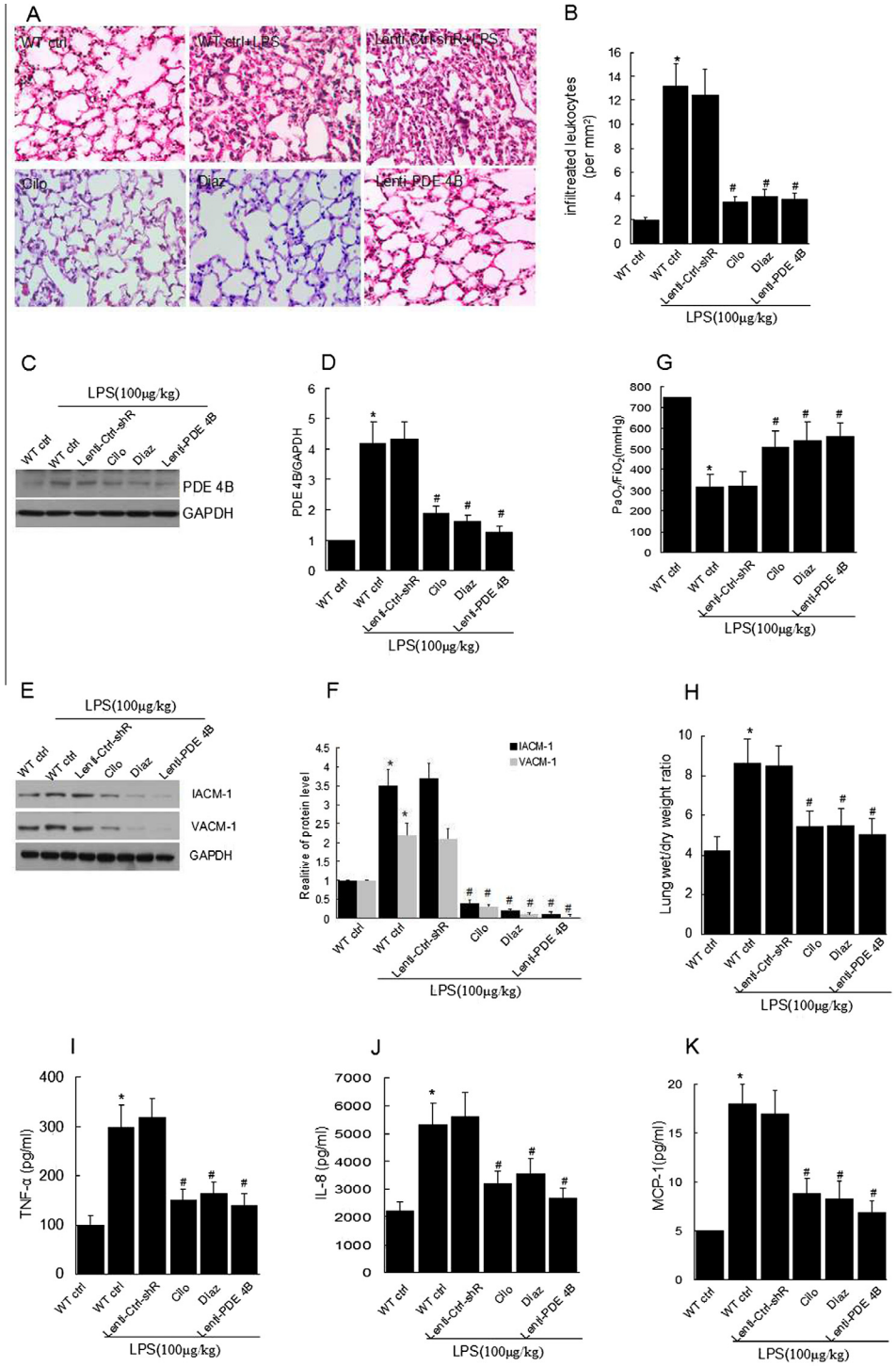

Fig. 4. Blockade of PDE4B inhibited lung inflammatory response in vivo. C57BL/6 mice were treated with Cilomilast (10 mg/kg) or Diazepam (10 mg/kg) or lentivirus vector targeting PDE4B (100 MOI/kg/day) or Lenti-Ctrl-shRNA E(100 MOI/kg/day) for 4 weeks, then challenged with LPS (100 μg/kg) for 6 h. DMSO was used as a vehicle control. Samples were collected after 24 h. (A) Representative photomicrographs of lung sections with H&E staining. Original magnification× 400. (B) Quantification of alveolar leukocytes infiltration (Data represent mean ± SD, $^{\#}P < 0.05$ vs. WT control; $^{*}P < 0.05$ vs. LPS alone. $n = 3$). (C) Representative Western blot of PDE4B induction in multiple regions of the lung slices treated with LPS. (D) Statistical data of PDE4B protein level (Data represent mean ± SD, $^{\#}P < 0.05$ vs. WT control; $^{*}P < 0.05$ vs. LPS alone. $n > 3$). (E) Representative Western blot of IACM-1 and VACM-1 induction in multiple regions of the lung slices treated with LPS. (F) Statistical data of IACM-1 and VACM-1 protein level (Data represent mean ± SD, $^{\#}P < 0.05$ vs. WT control; $^{*}P < 0.05$ vs. LPS alone. $n > 3$). (G) PaO_2/FIO_2 (P/F) ratio (Data represent mean ± SD, $^{\#}P < 0.05$ vs. WT control; $^{*}P < 0.05$ vs. LPS alone. $n > 3$). (H) Lung water changes (Data represent mean ± SD, $^{\#}P < 0.05$ vs. WT control; $^{*}P < 0.05$ vs. LPS alone. $n > 3$). (I–K) Cytokine protein levels were measured in BAL from mice. (I) TNF-α, (J) IL-8, (K) MCP-1 (Data represent mean ± SD, $^{\#}P < 0.05$ vs. WT control; $^{*}P < 0.05$ vs. LPS alone. $n > 3$).

was alveolar destruction, by contrast, lung architecture and leukocyte infiltration presented obviously remission in mice treated with PDE4B blockers or PDE4B shRNA Lentiviral Particles. Besides, blockade of PDE4B in mice also significantly inhibited polymorphonuclear neutrophil (PMN) infiltration in bronchoalveolar lavage (BAL) fluids (Fig. 4B). The levels of IL-8, TNF-α and MCP-1 from BAL

of mice treated with PDE4B blockers or PDE4B shRNA Lentiviral Particles were decreased obviously when compared with that of C57BL/6 wild-type mice(Fig. 4I–K). Consistent with these results, lung wet/dry ratios were decreased when compared with untreated group or normal control group (Fig. 4H), whereas the PaO_2/FIO_2 (*P*/*F*) ratios were elevated significantly in the mice pretreated with Cilomilast or Diazepam or PDE4B shRNA Lentiviral Particles (Fig. 4G). We also examined the protein expression of IACM-1 and VACM-1 in this model, and found that IACM-1 and VACM-1 were locked down in Lenti-PDE4B KO mice or mice treated with PDE4B blockers (Fig. 4E and F).

4. Discussion

Several reports have indicated that PDE4B may be involved in inflammation [7,8,10,21,22], However, which mechanism of action of PDE4B is critical for maintenance of vascular integrity has not been well understood. In the present study, we found that blockade of PDE4B limited lung vascular permeability and lung inflammation. To explore the molecular mechanisms, we analyzed the levels of proinflammatory cytokines in vitro and in vivo. Our data showed that PDE4B blockers or PDE4B knockout prevented the expression of LPS-induced proinflammatory cytokines including VCAM-1, ICAM-1, IL-8 and MCP-1.

Oxidative signaling and NF-κB activation were tightly linked with cellular responses [4]. We investigated that LPS-mediated NF-κB activation are ablated in PDE4B deletion. And, PDE4B knockout was parallel to the abrogation of NF-κB activation. And, we also found that LPS-induced ROS levels was suppressed by preventing the expression of PDE4B. We also examined the phosphorylation level of eNOS which had been supposed to play a crucial role in mediating the pathogenesis of inflammatory response and microvascular permeability. And, our data showed that PDE4B deletion promoted LPS-inhibited p-eNOS activity. Even, blockade of PDE4B prevented LPS-induced vascular leakage and pulmonary inflammation.

LPS is widely used to induce ALI in murine models [1–3]. And in our study, LPS was employed to establish the model of ALI in cells or in mice. LPS-challenged mice exhibit a typical pathological evidence of ALI, including increased inflammatory cytokine levels, higher vascular permeability, and alveolar fluid accumulation. However, blockade of PDE4B inhibited histological pathological signs of pulmonary injury, proinflammatory factors, lung wet/dry ratios and increased the PaO_2/FIO_2 ratio in the model of ALI.

In summary, blockade of PDE4B effectively suppresses proinflammatory factors and limits lung vascular permeability. Collectively, all the data indicates that PDE 4B is an aggressive target for anti-ALI.

Disclosure

We declare there is no conflicts of interest in the manuscript entitled.

Acknowledgments

This work was supported by Scientific and Technological Planning Project of Heilongjiang Province, China (No. GC09C409-3; No. GC12C305-5); Science and Technology Planning Project of Guangdong Province, China (2010A030100011-06); the Fundamental Research Funds for the Central Universities in China (No. 12ykpy26); Financial support by grants from the National Natural Science Foundation of China (No. 30972839).

Appendix A. Supplementary data

Supplementary data associated with this article can be found, in the online version, at http://dx.doi.org/10.1016/j.bbrc.2014.07.024.

References

[1] Jun Li, Li Zhao, Xie He, et al., Sinomenine protects against lipopolysaccharide-induced acute lung injury in mice via adenosine A_{2A} receptor signaling, PLoS One 8 (3) (2013) e59257.
[2] G. Wang, X. Huang, Y. Li, et al., PARP-1 inhibitor DPQ attenuates LPS-induced acute lung injury through inhibiting NF-κB-mediated inflammatory response, PLoS One 8 (11) (2013) e79757 (21).
[3] X. He, J.L. Hu, J. Li, et al., A feedback loop in PPARγ-adenosine A_{2A} receptor signaling inhibits inflammation and attenuates lung damages in a mouse model of LPS-induced acute lung injury, Cell Signal. 25 (9) (2013) 1913–1923.
[4] R.K. Gandhirajan, S. Meng, H.C. Chandramoorthy, et al., Blockade of NOX2 and STIM1 signaling limits lipopolysaccharide-induced vascular inflammation, J. Clin. Invest. 123 (2) (2013) 887–902.
[5] K. Komatsu, J.Y. Lee, M. Miyata, et al., Inhibition of PDE4B suppresses inflammation by increasing expression of the deubiquitinase CYLD, Nat. Commun. 4 (2013) 1684.
[6] M. Tauseef, N. Knezevic, K.R. Chava, et al., TLR4 activation of TRPC6-dependent calcium signaling mediates endotoxin-induced lung vascular permeability and inflammation, J. Exp. Med. 209 (11) (2012) 1953–1968.
[7] K.F. MacKenzie, D.A. Wallace, E.V. Hill, et al., Phosphorylation of cAMP-specific PDE4A5 (phosphodiesterase-4A5) by MK2 (MAPKAPK2) attenuates its activation through protein kinase A phosphorylation, Biochem. J. 435 (3) (2011) 755–769.
[8] S.L. Jin, M. Conti, Induction of the cyclic nucleotide phosphodiesterase PDE4B is essential for LPS-activated TNF-alpha responses, Proc. Natl. Acad. Sci. U.S.A. 99 (11) (2002) 7628–7633.
[9] T.L. Hwang, M.C. Tang, L.M. Kuo, et al., YC-1 potentiates cAMP-induced CREB activation and nitric oxide production in alveolar macrophages, Toxicol. Appl. Pharmacol. 260 (2) (2012) 193–200.
[10] B.E. Blackman, K. Horner, J. Heidmann, et al., PDE4D and PDE4B function in distinct subcellular compartments in mouse embryonic fibroblasts, J. Biol. Chem. 286 (14) (2011) 12590–12601.
[11] T. Keravis, F. Monneaux, I. Yougbaré, et al., Disease progression in MRL/lpr lupus-prone mice is reduced by NCS 613, a specific cyclic nucleotide phosphodiesterase type 4 (PDE4) inhibitor, PLoS One 7 (1) (2012) e28899.
[12] I. Yougbare, C. Morin, F.Y. Senouvo, et al., NCS 613, a potent and specific PDE4 inhibitor, displays anti-inflammatory effects on human lung tissues, Am. J. Physiol. Lung Cell. Mol. Physiol. 301 (4) (2011) L441–L450.
[13] S.W. Kim, D. Rai, M.R. McKeller, et al., Rational combined targeting of phosphodiesterase 4B and SYK in DLBCL, Blood 113 (24) (2009) 6153–6160.
[14] K.I. Jeon, X. Xu, T. Aizawa, et al., Vinpocetine inhibits NF-kappaB-dependent inflammation via an IKK-dependent but PDE-independent mechanism, Proc. Natl. Acad. Sci. U.S.A. 107 (21) (2010) 9795–9800.
[15] M. Sobczak, J. Dargatz, M. Chrzanowska-Wodnicka, Isolation and culture of pulmonary endothelial cells from neonatal mice, J. Vis. Exp. 46 (2010) e2316.
[16] H. Yang, L.Y. Huang, D.Y. Zeng, et al., Decrease of intracellular chloride concentration promotes endothelial cell inflammation by activating nuclear factor-κB pathway, Hypertension 60 (5) (2012) 1287–1293.
[17] S. El-Andaloussi, Y. Lee, S. Lakhal-Littleton, et al., Exosome-mediated delivery of siRNA in vitro and in vivo, Nat. Protoc. 7 (12) (2012) 2112–2126.
[18] Toru Aizawa, Heng Wei, J.M. Miano, et al., Role of phosphodiesterase 3 in NO/cGMP-mediated antiinflammatory effects in vascular smooth muscle cells, Circ. Res. 93 (2003) 406–413.
[19] W. Li, Y.P. Wang, L. Gao, et al., Resveratrol protects rabbit ventricular myocytes against oxidative stress-induced arrhythmogenic activity and Ca^{2+} overload, Acta Pharmacol. Sin. 34 (9) (2013) 1164–1173.
[20] E.W. Huang, S.J. Xue, Z. Zhang, et al., Vinpocetine inhibits breast cancer cells growth in vitro and in vivo, Apoptosis 17 (10) (2012) 1120–1130.
[21] S.D. Martina, M.S. Ismail, K.S. Vesta, Cilomilast: orally active selective phosphodiesterase-4 inhibitor for treatment of chronic obstructive pulmonary disease, Ann. Pharmacother. 40 (10) (2006) 1822–1828.
[22] K. Woyda, S. Koebrich, I. Reiss, et al., Inhibition of phosphodiesterase 4 enhances lung alveolarisation in neonatal mice exposed to hyperoxia, Eur. Respir. J. 33 (4) (2009) 861–870.